SAIMM

J. S. Afr. Inst. Min. Metall., vol. 92, no. 6.
Jun. 1992. pp. 159–168

Simulation of fracture growth around openings in highly stressed, brittle rock

by J.A.L. Napier* and M.W. Hildyard*

SYNOPSIS

The improved design of support systems and stoping strategies when changes in depth, stratigraphy, or mine layouts are considered must rely on the designer's fundamental understanding of the deformation mechanisms adjacent to underground openings so that he can extrapolate and predict expected mining conditions.

This paper presents a numerical approach to the modelling of the growth and interaction of mining-induced fractures near the edges of deep tabular excavations in brittle rock. Fractures are represented by displacement-discontinuity elements that are allowed to propagate according to prescribed growth rules. This procedure is justified by the reproduction of several features observed in laboratory simulations of fracturing around openings in blocks of rock subjected to uniaxial and biaxial compression.

An attempt is then made to explain some of the attributes of the fracture zone surrounding tabular stopes. Particular questions of interest are the sequence in which fractures form and are mobilized in front of the mining face, the effect of parting planes parallel to the plane of the excavation, and the distribution of stress parallel to the hangingwall and footwall.

SAMEVATTING

Die beter ontwerp van stutstelsels en afboustrategieë wanneer veranderinge in diepte, stratigrafie of mynuitleg oorweeg word, moet staatmaak op die ontwerper se fundamentele begrip van die vervormingsmeganismes langs die ondergrondse openinge sodat hy die verwagte mynboutoestande kan ekstrapoleer en voorspel.

Hierdie referaat bied 'n numeriese benadering van die modellering van die groei en interaksie van mynbougeïnduseerde breuke naby die kante van diep tafelvormige uitgrawings in bros gesteentes. Breuke word voorgestel deur verplasingsdiskontinuïteitelemente wat toegelaat word om volgens voorgeskrewe groeireëls voort te plant. Hierdie prosedure word geregverdig deur die reproduksie van verskeie aspekte wat waargeneem is in laboratoriumsimulasies van breuke om openings in rotsblokke wat aan uniaksiale en biaksiale druk onderwerp is.

Daarna word 'n poging aangewend om sommige van die eienskappe van die breuksone om tafelvormige afbouplekke te verklaar. 'n Paar interessante kwessies is die volgorde waarin breuke vorm en voor die mynboufront gemobiliseer word, die uitwerking van skeidingsvlakke parallel met die uitgrawingsvlak, en die spanningsverdeling parallel met die dak en vloer.

INTRODUCTION

A conceptual understanding of the nature of the fracture zone induced by tabular excavations in deep mines, established in the Witwatersrand and Orange Free State goldfields of South Africa, has been built up over a number of years. This knowledge has been compiled from the mapping of fracture exposures on the hangingwalls of stopes and on the sidewalls of gullies advanced ahead of the mining face, as well as from observations of fractures intersecting boreholes drilled from tunnels below stopes, at different angles into the stope face, and vertically into the hangingwall[1-7].

Most of these observations were made at depths exceeding 2000 m. In a perfectly elastic rockmass having a Young's modulus of 70 GPa, the critical half span, at which total closure of 1 m occurs in a parallel-sided panel, would typically be about 300 m at this depth. In layered rock strata, where parting planes parallel to the hangingwall and footwall of the excavations tend to be mobilized, and where inelastic fracturing occurs, the open span to be supported behind the mining face can be reduced to as little as 30 m. The predominant types of fracture that have been observed are illustrated schematically in Figure 1.

The type 1 fractures (forward dipping in the hangingwall with respect to the mining direction) appear to be extension fractures with no slip movements. The type 2 fractures (backward dipping in the hangingwall) are observed to have shear movements and often contain comminuted gouge material on the fracture interface. The spacing between the sheared fractures is irregular (of the order of a few metres), but they are considered usually to form in a quasi-static manner[4], as opposed to burst fractures associated with dynamic and unstable rock movements[8]. Some investigators[9] have suggested that fractures occurring in the type 2 orientation may, in fact, be initiated as extension fractures ahead of the stope face and are subsequently sheared as the mining face is advanced.

From the point of view of practical mine-support design, it is important to understand the evolution and effect of the stress state in the rockmass close to the advancing face. In particular, how does the stress state evolve as an excavation is established, and what mechanisms control the inherent stability or instability of the immediate hangingwall? This

* Chamber of Mines Research Organization, P.O. Box 91230, Auckland Park, 2006 Transvaal.
 SA ISSN 0038-223X/3.00 + 0.00. Paper received August 1991; revised paper received March 1992.

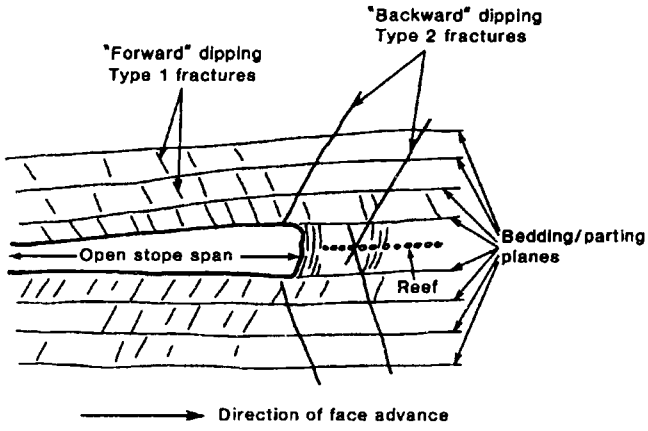

Figure 1—Vertical section through a tabular stope at great depth, illustrating the predominant types of fracture[4]

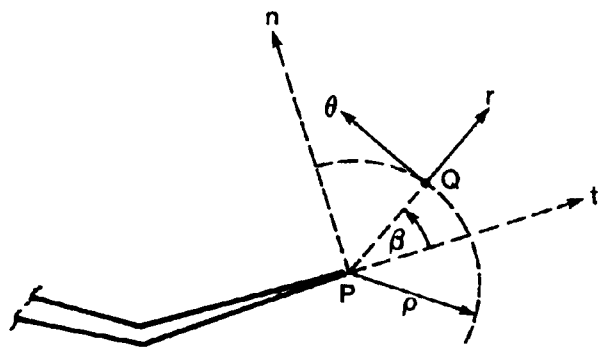

Figure 2—Selection of optimum growth angle, β, evaluated at a specified distance, p, from an existing crack tip, P

knowledge is a prerequisite to the adaptation of current support and stoping strategies, and ultimately offers the potential of manipulating fracture patterns to achieve improved stability and safety.

SIMULATION OF FRACTURE GROWTH

The fracture zone shown schematically in Figure 1 can be represented numerically by a set of fictitious cracks or dislocations in an elastic body, appropriate strain nuclei being used to reflect a jump in the displacement field on the opposite sides of each crack. This displacement-discontinuity method[10-14] can be extended to the modelling of fracture growth as a pseudo-static process if each crack tip is advanced incrementally in a direction that maximizes a specified growth criterion. Several criteria have been proposed, including local strain-energy density, angular tensile stress, energy-release rate, or combinations of Mode I and Mode II stress-intensity factors[14-19]. In this study, two basic modes of fracture in brittle rock are distinguished, namely extension or cleavage fracturing, and shear fracturing. Fracturing is assumed to continue from an existing crack tip if a specified failure criterion is met at a designated point ahead of the crack tip. The failure criterion is formulated in terms of the components of the local stress tensor at the designated point. The sign of the stress-tensor components is assumed to follow conventional elasticity theory, in which tensile stresses are positive and principal stresses are designated $\sigma_I \geq \sigma_{II} \geq \sigma_{III}$. To conform to geomechanics usage, *major*, *intermediate*, and *minor* principal stress components are defined respectively as

$$\begin{aligned} \sigma_1 &= -\sigma_{III} \\ \sigma_2 &= -\sigma_{II} \\ \sigma_3 &= -\sigma_I . \end{aligned} \qquad [1]$$

The point at which the specified failure criterion is to be evaluated is determined as follows. For the growth of an extension fracture, the local angular stress component, $\tau_{\theta\theta}$, is evaluated at points that are located at a fixed distance, ρ, from the tip of the growing crack, and the growth angle, β, at which $\tau_{\theta\theta}$ is a maximum (tension positive) is selected (Figure 2).

Shear growth is simulated by selection of the angle β at which the shear–stress obliquity or 'excess shear', τ_e, is a maximum. This is defined, where ϕ is the angle of internal friction, as

$$\begin{aligned} \tau_e &= |\tau_{r\theta}| + \tan\phi\tau_{\theta\theta} \; ; \tau_{\theta\theta} \text{ negative (i.e. compressive)} \\ \tau_e &= |\tau_{r\theta}| \qquad\qquad ; \tau_{\theta\theta} \text{ zero or positive (i.e. tensile).} \end{aligned} \qquad [2]$$

It is recognized that the process of shear growth comprises a complex sub-structure of linked fractures to form a shear zone of finite thickness. It is assumed that this macro-zone can be modelled as a displacement-discontinuity 'cut' in the medium, which has constitutive properties that can be made equivalent to appropriate friction and dilation angles applied at the discontinuity interface. In the present paper, it is assumed that the dilation angle associated with slip on contacting discontinuity surfaces is zero. These assumptions are justified from a comparison of simulated fracture patterns with observed fractures in physical models or near underground openings. It should be noted[20] also that, if criterion [2] is applied at a point in a compressive-stress field, the maximum excess shear stress occurs on conjugate planes parallel to the intermediate principal stress, σ_2, and inclined at angles $\pm\,\alpha$ to the major (compressive) principal stress direction, σ_1. The angle α is given by

$$\alpha = \pi/4 - \phi/2. \qquad [3]$$

For granular media, this angle is observed[21] and theoretically predicted[22,23] to be

$$\alpha = \pi/4 - (\phi + \psi)/4, \qquad [4]$$

where ψ is the dilation angle of the failing material. However, Vermeer[24] has argued that the Coulomb angle, α, given by equation [3] becomes more appropriate as the grain size of the material becomes smaller. This is also supported by observations of the inclinations of large-scale tectonic faults[25].

Once the optimum growth angle has been selected, fracture growth occurs if a specified failure criterion is met at the point Q situated at the distance ρ and the angle β ahead of the crack tip (Figure 2). Specific criteria corresponding to modes of tension and shear failure [20,26]

are shown in Figure 3. The tension criterion is such that failure will not occur if the confining stress, σ_3, exceeds about one-tenth of the major compressive stress, σ_1. A reduced slope is used for the shear-failure criterion to reflect the effects of increased confinement on the failure envelope. The intact shear strength, *So*, and the friction angle, ϕ, corresponding to each failure criterion are shown in brackets in Figure 3. In general, the appropriate criteria must be calibrated according to physical observations. The simplistic approach of evaluating stresses at a fixed distance ahead of a crack tip will be influenced by the shape function assigned to the crack element, but a more elaborate scheme can be justified only by a greater understanding of the crack-tip process-zone mechanics, particularly during the growth of shear fractures. Some judgement must also be exercised in the selection of crack-initiation criteria to allow for the formation of fractures at stress levels that may be below the failure strength of the rock.

The conceptual procedure outlined above for crack growth has been embodied in a computer program known as DIGS (Discontinuity Interaction and Growth Simulation). This program solves an incremental sequence of problems, each comprising an assembly of elements that are arranged in segment groups. Following a solution cycle, active segments are checked to determine whether further growth is possible at one or both ends of the segment. If growth can occur, additional elements are introduced automatically in appropriate spatial orientations, and the problem is re-solved. Certain segments can be specified as 'fixed' and are not extended. The results are stored on disc files, which can be interpreted from hard-copy printouts or a graphics-plotting facility, DIGSPLT. All elements have a linear variation of the displacement-discontinuity density, and are solved by collocation of stresses at two points within each element[19].

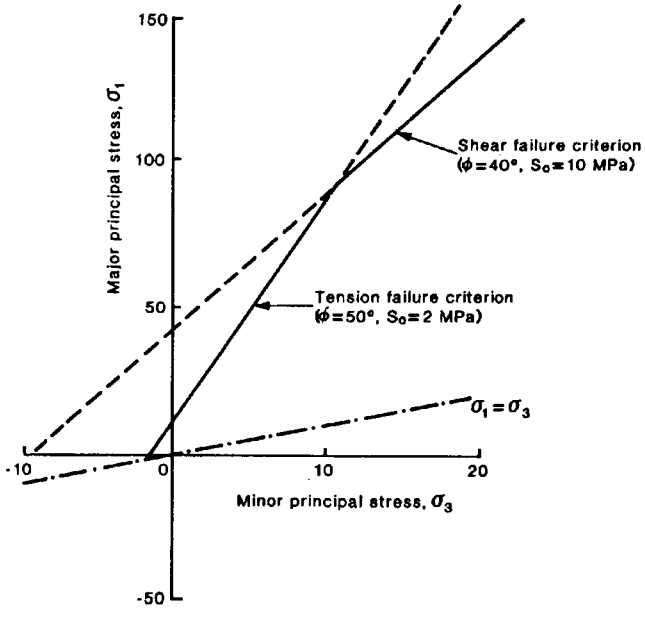

Figure 3—Stress criteria for the initiation of fractures in tension and shear modes

SMALL-SPAN OPENINGS IN MONOLITHIC ROCK

Maps of fracture patterns around small openings in laboratory-sized specimens of quartzite and sandstone have been presented by Gay[27,28]. In some of these experiments, the openings were enlarged laterally while the specimens were under either uniaxial or biaxial load. The major spans of each opening were perpendicular to the vertical loading direction. Figure 4 (reproduced from Gay's Figure 9[28]) shows the fracture patterns formed when openings in sandstone, subjected to different vertical-to-horizontal stress ratios, are enlarged progressively. Important observations made by Gay[28] were that domical fractures tended to form above the openings in specimens tested at low vertical-to-horizontal stress ratios, Figure 4(a), whereas at larger ratios large vertically orientated fractures tended to form at the edges of the openings when 'mined' to their maximum spans, as shown in Figures 4(b) and 4(c). Gay also noted that extension fractures formed in vertical orientations from both sides of the openings, at the centre, before the openings became enlarged. These can be seen in Figure 4.

A detailed simulation of the 'mining' sequences resulting in the patterns shown in Figure 4 is not attempted here. However, it is of interest to simulate the formation of fractures from the centre and from the edge of an opening in an infinite medium subjected to different biaxial loading ratios. The cross-section through the opening was chosen to have a width-to-height ratio of 5, and the Young's modulus, Poisson's ratio, and vertical far-field stress were set to 70 GPa, 0,2, and 60 MPa respectively. The horizontal far-field stress was set to 60, 30, and 0 MPa in cases (a), (b), and (c) shown in Figure 5; each diagram displays one of four symmetrical quadrants about the centre point of the excavation (marked +). Primary shear fractures (marked S1) were allowed to initiate from the edge of the opening, and a tension fracture (marked T) was allowed to initiate from the centre. Following two growth increments of the primary shear fracture (corresponding to 10 per cent of the half-span of the opening), a secondary shear fracture (S2) was allowed to form at the edge, and incremental growth was continued until the primary and secondary shear fractures reached the centre line, or ceased growing, or were terminated at a specified maximum number of increments. At that stage, a tertiary shear fracture (S3) was allowed to form and grow from the excavation edge. The principal stress orientations are also displayed in Figure 5.

These simulations provide a number of insights. The horizontal stress can be seen to play a strong role in determining the growth orientation of the shear fractures, which vary from a backward-dipping orientation in Figure 5(c) (zero σ_h) to a shallow arch in Figure 5(a) ($\sigma_v = \sigma_h$) as the horizontal stress is increased. The central tension fracture, T, does not form when the primitive horizontal stress equals the primitive vertical stress, Figure 5(a). It was noted from independent simulations that the central tension fracture would form in preference to a tension fracture initiating from the edge of the opening. It is also seen in Figure 5(b) ($\sigma_v = 2\sigma_h$) that the central tension fracture eventually bifurcated, after which growth was suppressed. This is qualitatively similar to the growth pattern seen in Figure 4(a).

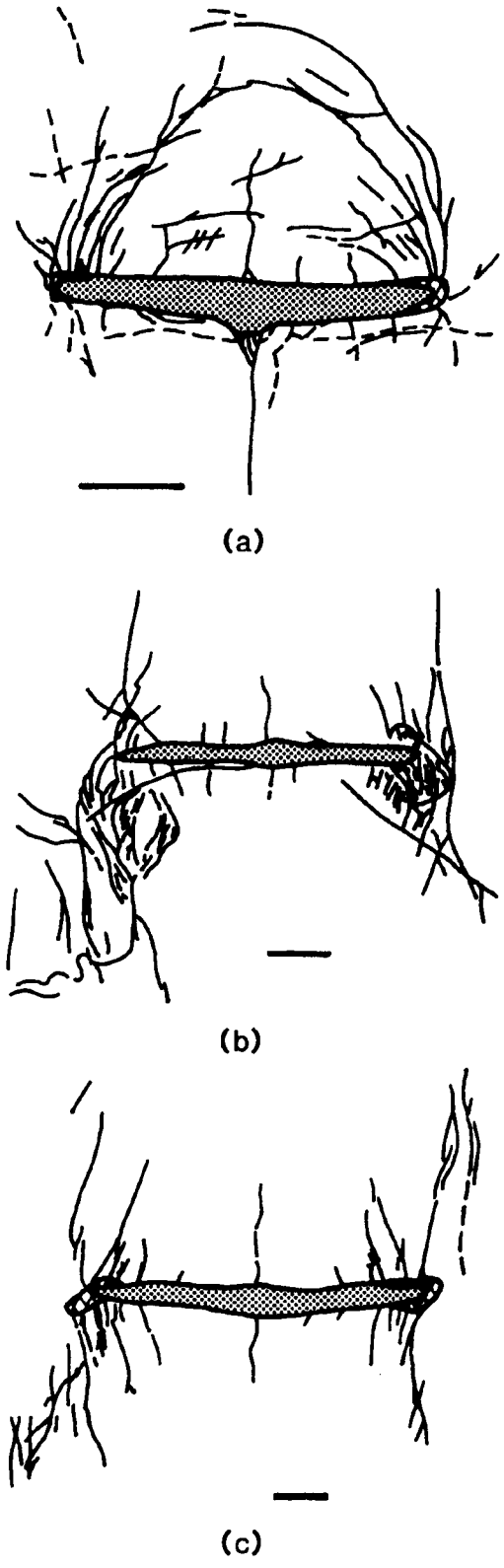

Figure 4—Detailed fracture maps[28] around openings in sandstone (scale bars = 10 mm)

(a) The interior of specimen C10, σ_v/σ_h = 1,95

(b) The front face of specimen C14, σ_v/σ_h = 2,5

(c) The front face of specimen C16, σ_v/σ_h = 2,6

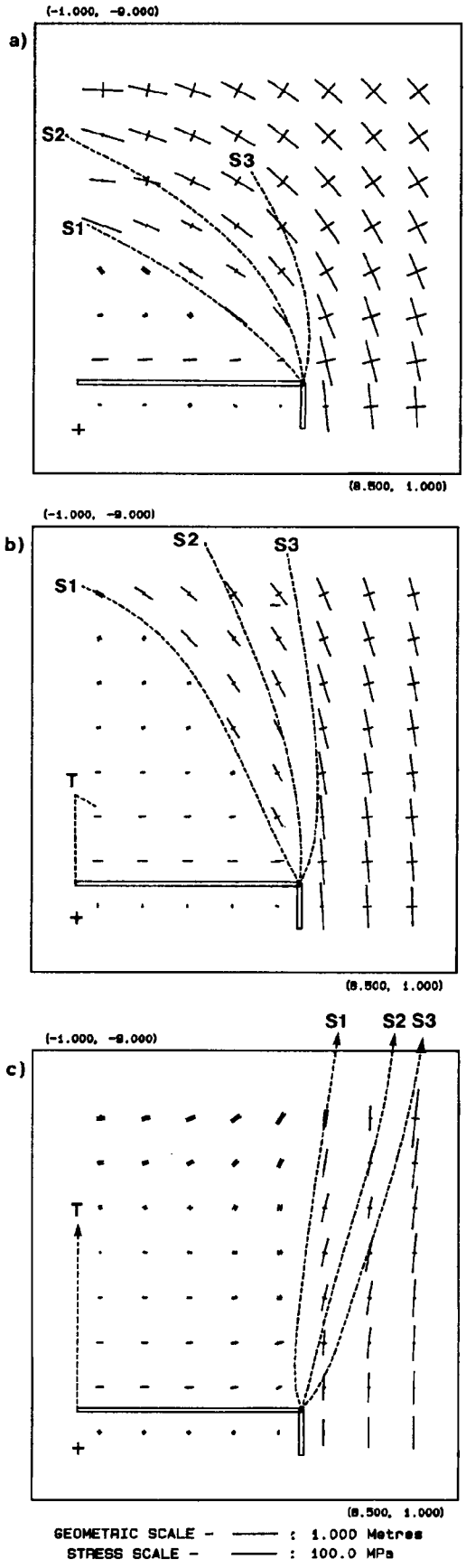

Figure 5—Shear and tension fracturing simulated near a rectangular opening in an infinite medium (compressive-stress tensor components are represented by a single line, and tensile components are represented by two parallel lines)

(a) σ_v/σ_h = 1; (b) σ_v/σ_h = 2; (c) σ_v/σ_h =∞

The formation of the secondary shear fracture S2 depends on the initial formation of the primary fracture S1 Similarly, the tertiary fracture S3 can form only once S2 has been initiated. The growth of S2 and S3 fractures is also limited where horizontal field stresses exist, Figures 5(a) and 5(b). It should be noted that the formation of high-angle fractures such as S1 can play a significant role in changing the condition in the immediate hangingwall of an excavation to a compressive state. This can be seen from an examination of the horizontal orientations of the major principal stress immediately above the roof of the excavations in Figure 5, and obviously has significant implications in the design of local stope support in deep mines and the effective self-stabilization of the hangingwall region[29].

SIMULATION OF BOREHOLE BREAKOUT

Fracturing in the sidewalls of boreholes drilled in highly stressed rock is often observed to occur as conical spalled regions on opposite sides of the hole, as shown in Figure 6. The orientation of this spalling is observed to be perpendicular to the major principal stress direction.

Spalling in this orientation is also observed in hollow rock cylinders subjected to axisymmetric loading on the outer surface and confined to plane strain in the axial direction. Ewy and Cook[31,32] have presented detailed experimental results of failure patterns induced at the inner surfaces of thick-walled hollow cylinders of Berea sandstone and Indiana limestone. The sequence of material failure and the failure mechanisms are extremely complicated. Ewy and Cook[31,32] and Zheng *et al.*[33] suggest that, near the surface of the hole, extension fractures can nucleate and extend initially parallel to the surface and then intersect the surface to form a spalled layer. Successive layers may then spall to form the typical breakout shape shown in Figure 6. Ewy and Cook[32] also noted that, deeper into the rock, confining pressures will check the growth of extension fractures, but groups of *enechelon* extension fractures may coalesce to form macro-shear failure zones.

The process of successive spalling of thin layers from the borehole surface was simulated by Zheng *et al.*[33] using a boundary-element computer code to model successive

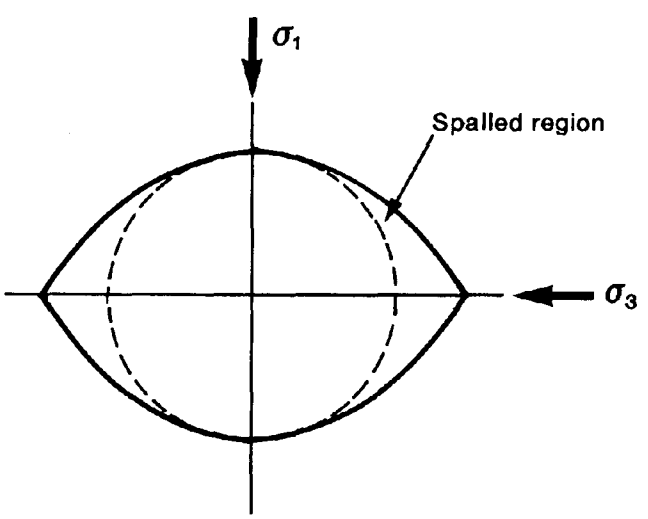

Figure 6—Borehole breakout orientation under biaxial loading[30]

changes in the shape of the opening. A stable profile, similar to that shown in Figure 6, is eventually achieved in which the induced stress in the surrounding material is such that the failure limit is nowhere exceeded. An alternative method, used in the present work, is to simulate a shear-fracture process that allows nucleation at the surface of a borehole (Figure 7). In Figure 7(a), shear fractures are nucleated simultaneously at equally spaced intervals marked S on the circumference, and form a characteristic breakout shape. No fractures are nucleated beyond an angle of 45 degrees from the horizontal stress axis. Based on the failure criterion depicted in Figure 3, the internal friction angle ϕ is 40 degrees and the initial growth angle is inclined at $45-\phi/2 = 25$ degrees to the circumference. In contrast to this, a single shear fracture nucleated preferentially at one point on the circumference, as shown by S1 in Figure 7(b), grows at a steeper angle after initiation and suppresses the formation of other shear fractures at the surface of the hole once it has been initiated. It is, however, possible to nucleate a secondary shear fracture, S2, from the first fracture. This mechanism of primary and secondary nucleation, and possibly successive subsidiary nucleation, appears to be similar to the fracture patterns depicted in Figure 5 of Ewy and Cook[31]. More generally, this demonstrates the potential viability of modelling the fracturing around tunnel-shaped excavations to predict failure mechanisms and to study the effect of support elements on the fractured region.

FRACTURES AHEAD OF STOPE FACES IN LAYERED STRATA

It is apparent from the observed and simulated fracture-growth patterns shown in Figures 4 and 5 respectively that shear fracturing at the edge of a narrow excavation in monolithic rock will tend to dip forwards towards the mining direction in the hangingwall region. The fracture orientation is controlled by the horizontal primitive stress and by the possibility of secondary fractures nucleating after the formation of an initial fracture. In particular, there is no numerical evidence that these fractures would form in a backward-dipping direction (Figure 1) or ahead of the stope-face position if the horizontal primitive stress is appreciably compressive.

However, the observations of underground fracturing[2-7,9] presented schematically in Figure 1 suggest that fracturing does initiate ahead of the stope face, and that shear or sheared fractures with backward-dipping orientations do occur. In assessing the differences between laboratory observations or simple numerical simulations and underground fracture patterns, one should note that the deep-level excavations considered here are advanced incrementally in small steps of approximately 1 m and are not formed instantaneously. The evolution of the fracture zone can, in general, be expected to affect the distribution of stress at a given mining span. An example of a particular mechanism that causes the horizontal stress component to be progressively increased is discussed by Kuijpers and Napier[29]. A second factor that can be expected to affect the formation of mining-induced fractures is the layered nature of the rock strata associated with the schematic fracture pattern shown in Figure 1.

Figure 8(a) shows the stress distribution near the end of a

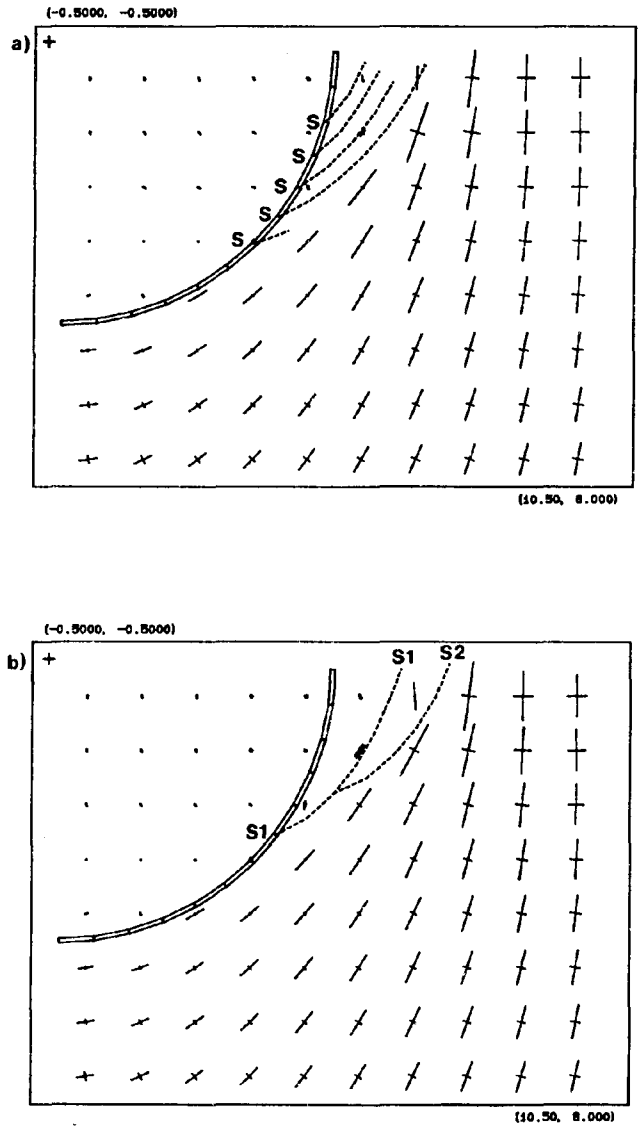

Figure 7—Simulated shear-fracture growth patterns from the surface of a circular hole loaded biaxially in the far field with a stress ratio of 2:1

(a) Simultaneous nucleation from several points on the circumference

(b) Nucleation from a single point on the circumference followed by secondary shear growth

narrow stope of 100 m span in an isotropic elastic rockmass. The continuation of the reef plane to the right of the stope face is shown as a single line and is modelled as a parting plane. No slip is observed to occur on this line. The primitive principal stresses in this case were chosen to be compressive in the vertical and horizontal directions, and to have absolute values of 60 and 30 MPa respectively. The elastic constants correspond to a Young's modulus of 70 GPa and a Poisson's ratio of 0,2. It has been suggested that the backward-dipping type 2 fractures (Figure 1) may initiate as extension fractures parallel to the direction of the major principal stress (King *et al.*)[9]. Although the major principal stresses shown ahead of the stope face in Figure 8(a) do show a 'backward' inclination, it is apparent that the minor principal stress is so large that extension fractures would not be expected to form in this orientation. It is also clear that a shear fracture propagating from the edge of the excavation would tend to be directed towards the region above the opening, as simulated in Figure 5(b). This corresponds qualitatively to the analogous situation of the expected tectonic shear-fault orientation near a vertically displaced basement block below a uniform overburden, as discussed by Mandl[25]. Conversely, Mandl argues that, in a multilayered overburden in which inter-layer slip can arise, the principal stresses will become more vertically oriented, and faulting can be expected to be oriented in the opposite sense ('backward' dipping in the terminology used here). The analogous mining situation is that the fractures at the stope face would tend to be backward dipping if multiple parting planes relieved the shear stress on layers parallel to the excavation. However, this mechanism will depend also on the average inter-layer spacing and the continuity in the horizontal direction of individual layers.

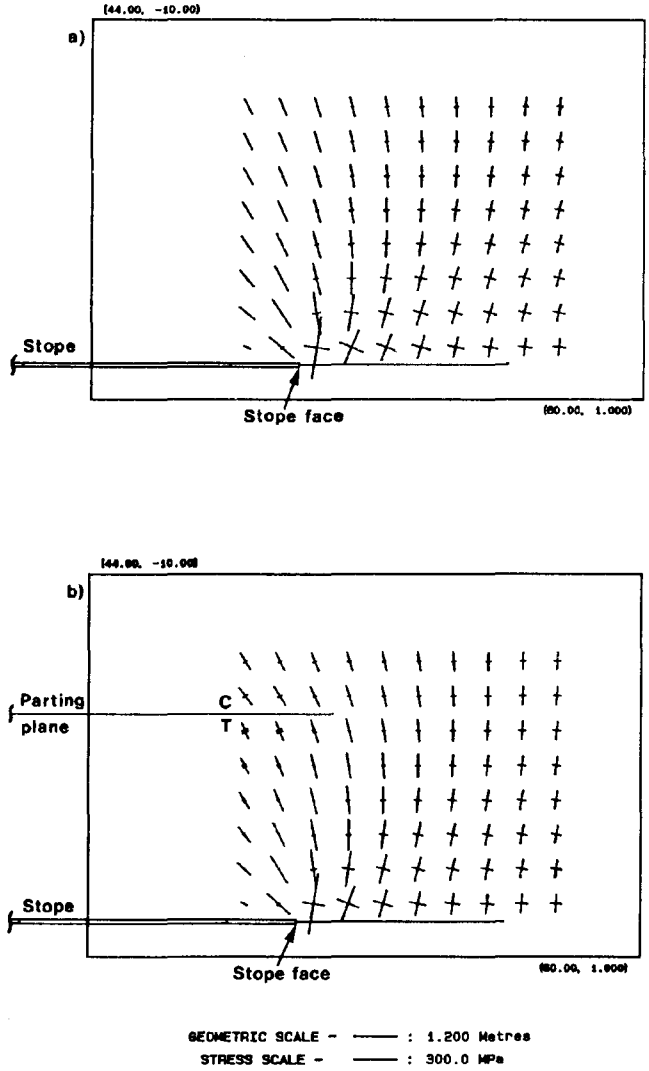

Figure 8—Stress distribution near the face of a panel 100 m in span in elastic rock (double bars represent tensile-stress components)

(a) No parting planes

(b) One parting plane 6 m above the panel

Figure 8(b) shows the effect of introducing parting planes with an interfacial friction angle of 30 degrees, 6 m above and 6 m below the stope. (The lower parting is not shown; in all the cases reported here, double symmetry is used above and below the stope and about the vertical centreline.) From a comparison of Figures 8(b) and 8(a), it can be seen that tensile stresses are induced below the interface in the region marked T, and the minor principal stress becomes more compressive above the parting plane in the region marked C. These changes in induced stress are particularly significant with respect to the propagation of the fracture in the vicinity of the interface. Fractures growing towards the interface from the stope are likely to be terminated by the 'jump' in horizontal stress from tension to compression. Conversely, extension or cleavage fractures could be initiated below the interface in the region marked T.

Figure 9(a) demonstrates the effect of introducing multiple parting planes spaced vertically at 2 m intervals, showing alternating regions of compression and tension above and below each interface in the region immediately behind the advancing stope face. With an interface friction angle of 30 degrees, it is found that the parting planes are not mobilized further than 1 m ahead of the vertical line above the position of the stope face. If Figure 9(a) is compared with Figure 8(a), it is apparent that the principal stresses ahead of the stope face are not very strongly affected by the parting planes. Consequently, the orientation of a shear fracture initiated at the stope face, and marked S1 in Figure 9(b), tends to grow over the open area as in the simulations shown in Figure 5(b). However, this fracture will be interrupted by the parting plane. A secondary shear fracture, marked S2 in Figure 9(b), grows initially towards the solid region but is forced to extend almost vertically in the presence of the parting planes, rather than in the orientation of S2 shown in Figure 5(b). If conjugate pairs of fractures initiate ahead of the stope face near the reef plane, it is apparent that the forward-dipping member of the pair is more likely to be interrupted by mobilized parting planes than the other member, which can grow towards the solid region ahead of the stope face.

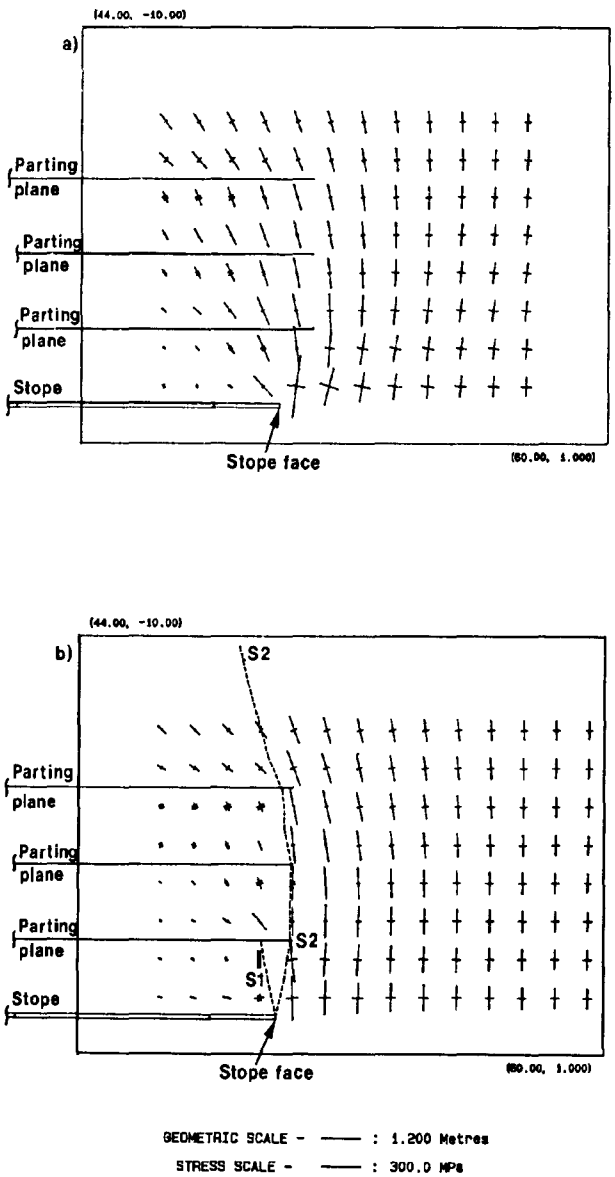

Figure 9—Stress induced by discontinuities near a stope face
(a) Multiple parting planes
(b) Growth of shear fractures from the stope face

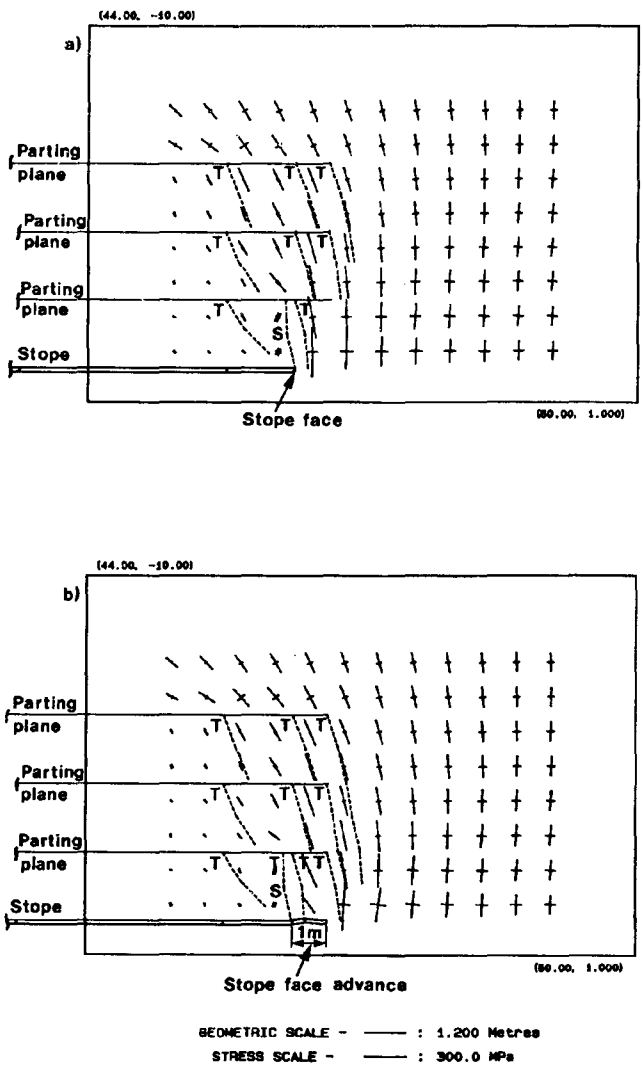

Figure 10—(a) Growth of extension fractures from the interfaces of parting planes
(b) Further growth following a mining step

The presence of parting planes may assist the nucleation of extension fractures. Figure 10(a) shows the growth of multiple extension fractures (T) from the lower side of the parting-plane interfaces. The spacing and number of fractures was chosen arbitrarily. In addition, a shear fracture, S, was allowed to form at the stope face. The direction of fracture growth is shown in Figure 10(a): all the extension fractures tend to follow the directions of major principal stress and terminate when the minor principal stress becomes sufficiently large, as determined by the initial portion of the failure envelope specified in Figure 3. Growth ahead of the stope face is seen to terminate 2 to 3 m above the reef plane. Following a mining step in which the stope face is suddenly advanced by 1 m, the extension fractures propagate further and may intersect the stope hangingwall, Figure 10(b). The forward-dipping orientation shown in Figures 10(a) and (b) is in general agreement with that observed for extension fractures underground. It must be noted that the patterns shown in Figure 10 resulted from a single-step excavation, rather than from an evolutionary mining process.

FRACTURE INITIATION AHEAD OF THE STOPE FACE

Observations from boreholes drilled into the advancing faces of deep-level tabular excavations suggest that fracturing initiates some distance ahead of the face (up to 10 m) depending on the field stress level[3,5]. Computer simulations of narrow openings that are created suddenly in an unfailed medium indicate that failure is initiated at the edges of the openings where extreme stress gradients exist. A mechanism that would allow failure to occur ahead of the stope face is demonstrated in Figure 11. Figure 11(a) shows the initial situation where a shear fracture and two extension fractures, similar to those formed furthest ahead of the stope face in Figure 10(b), are allowed to initiate. They are marked S1, and T1 and T2 respectively in Figure 11(a). A single line represents the continuation of the reef plane to the right of the stope face. This is modelled as a parting plane, but no slip is observed to occur on this line. If the stope face is advanced to intersect the extension fracture T2, considerable slip (not shown here) is induced on fracture T2, creating a block bounded by the upper parting plane, fracture T2, and the stope hangingwall. This, in turn, tends to reduce the horizontal stress in the region behind the fracture over the mined area, Figure 11(b). This effectively increases the mining width (in this case to 6 m above and 6 m below the original stope horizon), allowing multiple shear fractures to be formed ahead of the stope face in the orientation shown in Figure 11(b). (Shear fractures, S2, S3, etc., were allowed to initiate at 1 m intervals ahead of the face.) No fracturing was found to initiate beyond the fracture marked S6 in Figure 11(b). A further series of four mining-step increments were simulated, extending the stope by a distance of 4 m, with the resulting fracture-growth patterns shown in Figure 11(c). Here, it is interesting to note that, although fractures S3, S4, S5, and S6 all grow, no further fracturing is introduced ahead of the final face position at the root of the fracture marked S6. This behaviour is also observed if the parting plane is extended to the right of the limiting position shown in Figure 11(c) and if fractures S2 and S3

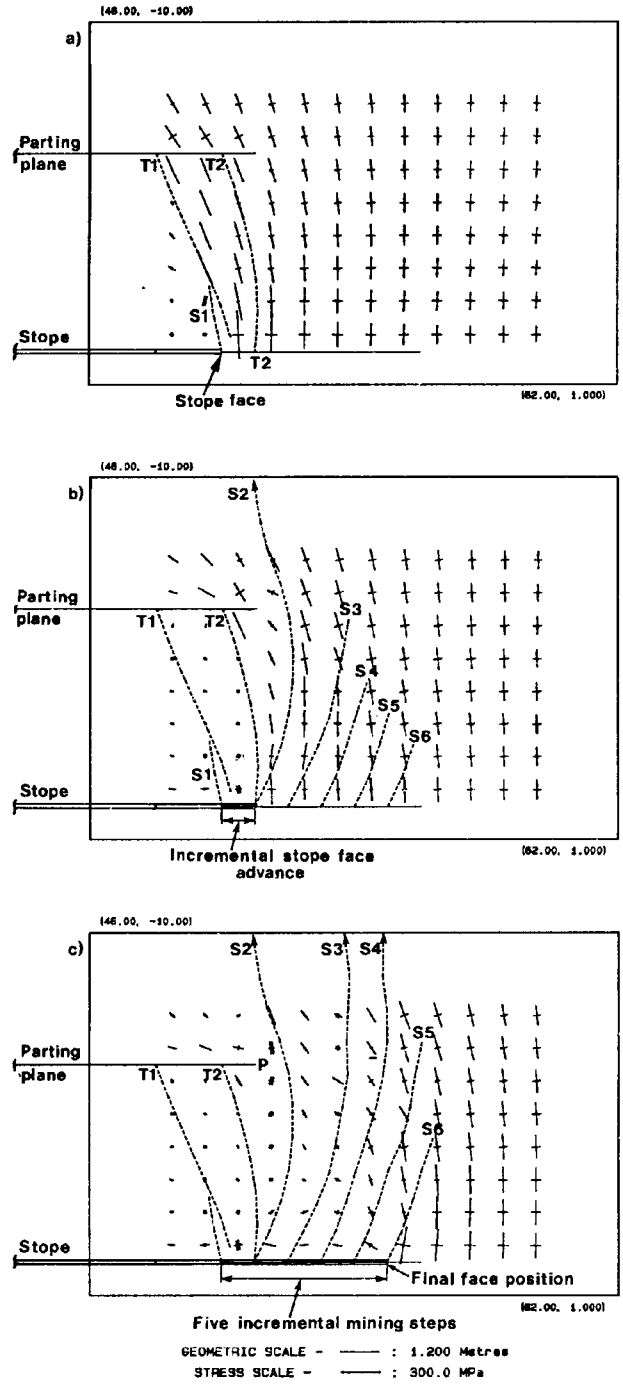

Figure 11—Effective increase in stoping width
(a) Extension fractures induced ahead of the stope face
(b) Intersection with mining step and secondary shear growth
(c) Additional mining steps

are allowed to intersect the parting plane. It has not yet been confirmed whether stress conditions similar to those shown in Figure 11(a) will be re-established, allowing a reduction of horizontal compressive stress and a repeated cycle of fracture initiation ahead of the mining face, as in Figures 11(b) and (c).

The concept of an 'effective stope width' was also proposed by Brummer[7], who employed a limit equilibrium model of interlocking rock wedges to model the vertical stress distribution ahead of the stope face. The simulations

presented in Figure 11 provide a means of generating such a block structure explicitly, but indicate that this structure can vary in a complicated manner as the mining sequence is evolved. In particular, it can be speculated that the effective stope width may be cyclic in nature, increasing and reducing as the mining face advances. Further studies of the evolution of fracturing are planned in which the simulation method will be enhanced to allow growing fractures to intersect existing discontinuities and parting planes.

CONCLUSIONS

An encouraging correspondence can be achieved between simulated fracture growth and laboratory-scale physical models of fracturing near narrow slot-like excavations and circular openings. The simulation of actual mining-induced fracturing is far more speculative but highlights the importance of geometrical features such as parting planes. Specific conclusions that can be reached are as follows.

(1) The primitive horizontal-to-vertical stress ratio controls the orientation of fracturing in monolithic (unlayered) material near the edges of slot-shaped openings. As the horizontal stress is increased, shear fractures initiating from the edges of the openings curve back over the opening to form domical structures, as reflected in physical modelling tests[28]. At zero horizontal stress, shear fractures tend to grow in a vertical orientation with respect to the horizontal opening.

(2) Multiple fractures can initiate at the edges of openings in monolithic material, but are formed in sequence at progressively steeper forward-dipping angles with respect to the major axis of the opening projected into the solid region.

(3) In single-step loading of small-span slot-shaped openings, tension fracturing is initiated preferentially at the centre of the opening, and effectively suppresses the formation of tension fractures that may initiate at the edges of the opening. The formation of the central tension fracture is itself suppressed when the horizontal primitive stress is increased sufficiently relative to the vertical primitive stress. This has obvious implications in the design of the support strategy to be employed in small-span ledging stopes.

(4) Parting planes can play a role in allowing extension fractures to initiate in the solid region above the edge of a tabular opening. In particular, the mobilization of parting planes can allow regions of strong tensile stress to be formed on the lower side of the parting-plane interface, which can encourage the nucleation of extension fractures dipping forward at about 80 degrees in the hangingwall.

(5) Mobilization of parting planes near the stope face can form a barrier to the growth of shear fracture, depending on the orientation of the fractures. For example, if conjugate fractures are formed in the reef plane ahead of the stope face, one member of the pair will tend to dip backwards above the reef plane, and can grow uninterruptedly into the solid region. The other member will be in a forward-dipping orientation and will tend to be interrupted by mobilized parting planes.

(6) In addition to this mechanism, mobilization of multiple parting planes parallel to the reef plane will allow shear stresses to be relaxed and cause the major principal stress to be tilted to an orientation nearly normal to the reef plane, in the region above the stope face. This, in turn, will favour the formation of backward-dipping fractures.

(7) Fracturing in the solid region ahead of the current edge of the opening is strongly affected by the horizontal stress parallel to the roof and floor of the opening. If this stress is reduced over an 'effective' stope width larger than the physical mining height, shear fractures can be formed ahead of the actual stope face at orientations observed *in situ* (backward-dipping in the hangingwall with respect to the mining direction). A mechanism leading to an effective widening of the stope width is demonstrated in Figure 11, but it has not been shown whether this condition would be repeated as mining progresses.

In general, the simulation of fracture formation becomes considerably more difficult when the boundary surfaces of the problem are altered progressively as in the incremental enlargement of mine openings. The current implementation of this procedure in the computer code DIGS requires considerable user insight in the selection of fracture-growth criteria and the specification of initial fracture-growth locations. Further limitations are imposed by the modeller's inability to model fracture intersection processes automatically during fracture growth, although the modeller can fix specific junctions. It would seem, however, that this approach could provide insight into the interpretation of observed mining-induced fracture patterns, as well as aiding the interpretation of failure mechanisms in physical modelling experiments.

ACKNOWLEDGEMENTS

The results reported here form part of the research programme into rockmass behaviour carried out by the Chamber of Mines Research Organization. The authors thank the Chamber of Mines for permission to publish this paper, and specifically thank Dr N.C. Gay and Mr A.J. Jager of the Rock Engineering Division for many helpful suggestions and insights, and Dr P.A. Cundall for several useful comments.

REFERENCES

1. KERSTEN, R.W.O. Report on Chamber of Mines Project No. 111/64/10108. Transvaal and Orange Free State Chamber of Mines Research Organization, 1964.
2. ADAMS, G.R., JAGER, A.J., and ROERING, C. Investigation of rock fracture around deep-level gold mine stopes. *Proceedings 22nd U.S. Symposium on Rock Mechanics*. Boston (USA), Massachussetts Institute of Technology, 1981. pp. 213-218.
3. ADAMS, G.R., and JAGER, A.J. Petroscopic observations of rock fracturing ahead of stope faces in deep-level gold mines. *J.S. Afr. Inst. Min. Metall.*, vol. 80, no. 6. 1980. pp. 204-209.
4. JOUGHIN, N.C., and JAGER, A.J. Fracture of rock at stope faces in South African gold mines. *Proceedings of a Symposium on Rockbursts: Prediction and Control*. London, Institution of Mining and Metallurgy, 1984. pp. 53-66.
5. LEGGE, N.B. Rock deformation in the vicinity of deep gold mine longwall stopes and its relation to fracture. University of Cardiff, Ph.D. thesis, 1984.
6. BRUMMER, R.K., and RORKE, A.J. Mining induced fracturing around deep gold mine stopes. Chamber of Mines of South Africa Research

Organization, unpublished report, 1984.
7. BRUMMER, R.K. Fracturing and deformation at the edges of tabular gold mining excavations and the development of a numerical model describing such phenomena. Rand Afrikaans University, Johannesburg, Ph.D. thesis, 1988.
8. GAY, N.C., and ORTLEPP, W.D. Anatomy of a mining-induced fault zone. *Bull. Geol. Soc. Am.*, vol. 90. 1979. pp. 47-58.
9. KING, R.G., JAGER, A.J., ROBERTS, M.K.C., and TURNER, P.A. Rock mechanics aspects of stoping without back-area support. Chamber of Mines of South Africa Research Organization, unpublished report, 1989.
10. RONGVED, L. Dislocation over a bounded plane area in an infinite solid. *J. Appl. Mech.*, vol. 24. 1957. pp. 252-254.
11. BERRY, D.S. An elastic treatment of ground movement due to mining. 1. Isotropic ground. *J. Mech. Phys. Solids.*, vol. 8. 1960. pp. 280-292.
12. SALAMON, M.D.G. Elastic analysis of displacements and stresses induced by the mining of seam or reef deposits. *J.S. Afr. Inst. Min. Metall.*, vol. 64, pt 1. 1963. pp. 128-149.
13. CROUCH, S.L. Solution of plane elasticity problems by the displacement discontinuity method. *Int. J. Numer. Meth. Engng*, vol. 10. 1976. pp. 301-343.
14. CORNET, F.H. Comparative analysis by the displacement-discontinuity method of two energy criteria of fracture. *J. Appl. Mech.*, vol. 46. 1979. pp. 349-355.
15. VANDAMME, L., and CURRAN, J.H. A three-dimensional hydraulic fracturing simulation. *Int. J. Numer. Meth. Engng*, vol. 28. 1989. pp. 909-927.
16. LIN, J., and PARMENTIER, E.M. Quasistatic propagation of a normal fault: A fracture mechanics model. *J. Struct. Geol.*, vol. 10. 1988. pp. 249-262.
17. OLSON, J., and POLLARD, D.D. Inferring stress states from detailed joint geometry. *Key questions in rock mechanics*. Rotterdam, Balkema, 1988. pp. 159-167.
18. MARTEL, S.J., and POLLARD, D.D. Mechanics of slip and fracture along small faults and simple strike–slip fault zones in granitic rock. *J. Geophys. Res.*, vol. 94, no. B7. 1989. pp. 9417-9428.
19. NAPIER, J.A.L. Modelling of fracturing near deep level gold mine excavations using a displacement discontinuity approach. *Mechanics of jointed and faulted rock*. Rossmanith (ed.). Rotterdam, Balkema, 1990. pp. 709-715.
20. JAEGER, J.C., and COOK, N.G.W. *Fundamentals of rock mechanics*. 3rd ed. London, Chapman & Hall, 1979.
21. ARTHUR, J.R.F., DUNSTON, T., AL-ANI Q.A.J.L., and ASSADI, A. Plastic deformation and failure in granular media. *Gèotechnique*, vol. 27. 1977. pp. 53-74.
22. VARDOULAKIS, I. Shear band inclination and shear modulus of sand in biaxial tests. *Int. J. Numer. Analyt. Meth. Geomech.*, vol. 4. 1980. pp. 103-119.
23. VERMEER, P.A., and DE BORST, R. Non-associated plasticity for soil, concrete and rock. *HERON*, vol. 29. 1984. pp. 1-64.
24. VERMEER, P.A. The orientation of shear bands in biaxial tests. *Gèotechnique*, vol. 40. 1990. pp. 223-236.
25. MANDL, G. *Mechanics of tectonic faulting*. Amsterdam, Elsevier, 1988.
26. ROEST, J.P.A., and GRAMBERG, J. Cyclic processes of fracture and failure around deep-level longwall stopes. *Static and dynamic considerations in rock engineering*. Brummer (ed.). Rotterdam, Balkema, 1990. pp. 265-272.
27. GAY, N.C. Fracture growth around openings in thick-walled cylinders of rock subjected to hydrostatic compression. *Int. J. Rock Mech. Min. Sci. & Geomech. Abstr.*, vol. 10. 1973. pp. 209-233.
28. GAY, N.C. Fracture growth around openings in large blocks of rock subjected to uniaxial and biaxial compression. *Ibid.*, vol. 13. 1976. pp. 231-243.
29. KUIJPERS, J.S., and NAPIER, J.A.L. The effect of loading history on stress generation due to inelastic deformations around deep-level tabular stopes. *J. S. Afr. Inst. Min. Metall.*, vol. 91. 1991 pp. 183-194.
30. LEEMAN, E.R. The measurement of stress in rock: Part I. The principles of rock stress measurements. *Symposium on Rock Mechanics and Strata Control in Mines*. Johannesburg, South African Institute of Mining and Metallurgy, 1965. pp. 248-284.
31. EWY, R.T., and COOK, N.G.W. Deformation and fracture around cylindrical openings in rock. I. Observations and analysis of deformations. *Int. J. Rock Mech. Min. Sci. & Geomech. Abstr.*, vol. 27. 1990. pp. 387-407.
32. EWY, R.T., and COOK, N.G.W. Deformation and fracture around cylindrical openings in rock. II. Initiation, growth and interaction of fractures. *Ibid.*, pp. 409-427.
33. ZHENG, Z., KEMENY, J., and COOK, N.G.W. Analysis of borehole breakouts. *J. Geophys. Res.*, vol. 94, no. B6. 1989. pp. 7171-7182.

Carbon-concentration measuring unit*

An innovative metallurgical instrument that enables continuous on-line measurements of the carbon concentration in carbon-in-pulp (CIP) adsorption tanks in the gold-mining industry has been launched by the Electronics Division of Debex (Pty) Ltd.

Branded the Debex C² Meter†, the carbon-concentration meter enables precise on-line measurement for the first time of the carbon concentration levels during the gold-recovery process, making possible significant improvements and cost savings in metallurgical gold-recovery plants.

The instrument was developed by Mintek after five years of in-depth research and development. Debex, as a leading manufacturer of process-control instrumentation in mining applications, was selected to manufacture and market the equipment.

Using ultrasonics to measure mixtures of pulp and carbon, the dip-in type instrument is a major improvement on the method currently used on mines, in which several 1-litre grab samples are taken three to four times per day for analysis in a laboratory, which is a cumbersome and time-consuming method.

The new unit provides continuous and reliable measurement of carbon concentration with an accuracy guaranteed to within 2,5 g/l over the operating range. The meter features user-friendly operating procedures, and has an output signal for direct comunication with process instrumentation in the control room. The probe is robust in construction, and extensive field testing has shown it can withstand prolonged exposure to harsh operational environments.

Debex Electronics Manager, John Williams, points out that, prior to the development of this equipment, the accurate measurement of carbon concentration levels in CIP operations was a major problem because the measurement technology simply did not exist. 'Now for the first time, this measuring device allows the plant metallurgist to monitor the carbon-in-pulp process by using off-the-shelf instrumentation. This enables gold plants to operate at higher efficiency levels and more cost effectively.'

Debex is currently developing a C² unit, which will be capable of the simultaneous monitoring of multiple probes.

* Issued by De Beers Industrial Diamond Division, P.O. Box 916, Johannesburg 2000.

† Debex C² Meter is a trade mark of Debex (Pty) Ltd.